Kovove Mater. 49 2011 1–9
DOI: 10.4149/km_2011_1_1

Towards superstrength of nanostructured metals and alloys, produced by SPD

R. Z. Valiev[1*], N. A. Enikeev[1], T. G. Langdon[2,3]

[1] *Institute of Physics of Advanced Materials, Ufa State Aviation Technical University, 12 K. Marx Str., Ufa 450000, Russia*
[2] *Departments of Aerospace & Mechanical Engineering and Materials Science, University of Southern California, Los Angeles, CA 90089-1453, U.S.A.*
[3] *Materials Research Group, School of Engineering Sciences, University of Southampton, Southampton SO17 1BJ, U.K.*

Received 20 August 2010, received in revised form 23 September 2010, accepted 24 September 2010

Abstract

The metals and alloys subjected to severe plastic deformation can possess not only ultrafine-grained (UFG) structure but also specific nanostructural features, such as non-equilibrium grain boundaries, nanotwins, grain boundary segregations and nano particles. The authors consider in the present work the role of these features in exhibition of high strength of nanostructured metals and alloys. In particular, it is demonstrated that the presence of grain boundary segregations and non-equilibrium boundaries can result in yield stress values that considerably exceed those predicted from the Hall-Petch relation for the given materials.

K e y w o r d s: severe plastic deformation (SPD), bulk nanostructured metals and alloys, superstrength, grain boundaries, segregations

1. Introduction

Nanostructuring is the new and promising way to enhance the properties of metals and alloys for advanced structural and functional application [1]. To date, it is well established that bulk nanostructured materials (BNM) can be produced successfully via microstructural refinement using severe plastic deformation (SPD), i.e. heavy straining under high imposed pressure [2]. SPD processing is an attractive procedure for many advanced applications, as it allows enhancing significantly properties of commonly used metals and alloys.

Since the pioneering work on producing UFG materials by SPD processing [3], two SPD techniques have attracted close attention and have lately experienced further development [2]. These techniques are high-pressure torsion (HPT) and equal-channel angular pressing (ECAP). For the last 10–15 years there appeared a wide diversity of new SPD techniques: for example, accumulative roll bonding (ARB), multi-axial forging, twist extrusion and others (see for example [2] for a more comprehensive review). Nevertheless, processing by HPT and ECAP has remained the most popular approach and recently this has acquired a new impulse for development through the modification of conventional die-sets and demonstrations that new opportunities are now available for involving these procedures in industrial processing, e.g. using ECAP with parallel channels and continuous ECAP-Conform [4].

Grain refinement is well known to result in strength enhancement of metals and alloys, with the experimental relation between yield strength σ_y and a mean grain size d described by the Hall-Petch relationship [5, 6]. However, for nanosized grains (20–50 nm) these relations are reported to be violated so that the Hall-Petch plot deviates from linear dependence at lower stress values and its slope k_y often becomes negative. In recent years this problem has been widely analysed in both experimental and theoretical studies [7, 8]. At the same time, Hall-Petch relationship breakdown is not observed in ultrafine-grained (UFG) materials with a mean grain size of 100–1000 nm usually produced by SPD processing. Moreover, recently we have shown that UFG alloys can exhibit a considerably higher strength than the Hall-Petch rela-

*Corresponding author: tel./fax: +7 347 2733422; e-mail address: rzvaliev@mail.rb.ru

tionship predicts for the range of ultrafine grains [9–11]. The nature of such superstrength may be associated with another nanostructural features (dislocation substructures, nanophase particles and segregations, nanotwins, etc.) which could be observed in the SPD-processed metals and alloys [9, 11].

In recent years in our laboratory in close collaboration with colleagues and partners there were performed a number of investigations of unusual mechanical performance of SPD-processed Al and Ti alloys as well as in several steels [9–13]. The present study deals with consideration and investigation of manifestation and nature of superstrength, which was observed in these nanostructured materials.

2. Experimental

The objects of this research were commercial Al alloys 1570 (Al-5.7Mg-0.32Sc-0.4Mn, wt.%), 7475 (Al-5.7Zn-2.2Mg-1.6Cu-0.25Cr, wt.%), Ti (Grade 4) and Armco-Fe [9, 12–14]. In order to obtain a UFG structure, solid-solute alloys were subjected to HPT and ECAP. For HPT-processing the applied pressure of 6 GPa and 20 rotations were used to process the alloys. The produced samples had the form of discs with a diameter of 20 mm and 0.6 mm in thickness, which are well suited for mechanical tests. ECAP processing has been performed with the dies of 10 and 20 mm in diameter [4].

The structural characterization was performed by transmission electron microscopy (TEM), X-ray diffraction (XRD) and atom probe tomography (APT). A mean grain size and a grain size distribution were estimated from TEM dark-field measurements in torsion plane over more than 350 grains from an area situated at the middle of an HPT disc radius. Selected-area electron diffraction (SAED) patterns have been taken from the area of 1.3 μm in diameter. XRD was performed with a Pan Analytical X'Pert diffractometer using Cu Kα radiation (50 kV and 40 mA). The lattice parameter a for the initial and HPT-processed alloys was calculated according to the Nelson-Riley extrapolation method [15]. Tensile tests have been precisely performed using a laser extensometer at room temperature with a strain rate of $10^{-4}\,s^{-1}$ on a computer-controlled testing machine operating with a constant displacement of the specimen grips. Strength characteristics were estimated by testing samples with a gage of $2.0 \times 1.0 \times 0.4\,mm^3$.

3. Results and discussion

3.1. Nanostructures in SPD-processed metals and alloys

Although it is possible to achieve a nanocrystalline structure with a grain size less than 100 nm in a number of metals and alloys by means of HPT [16, 17], for SPD processing by ECAP and HPT it is typical to form ultrafine-grained structures with mean grain sizes within the submicrometer range so that, typically, the grain sizes are ∼ 100–500 nm [4]. How-

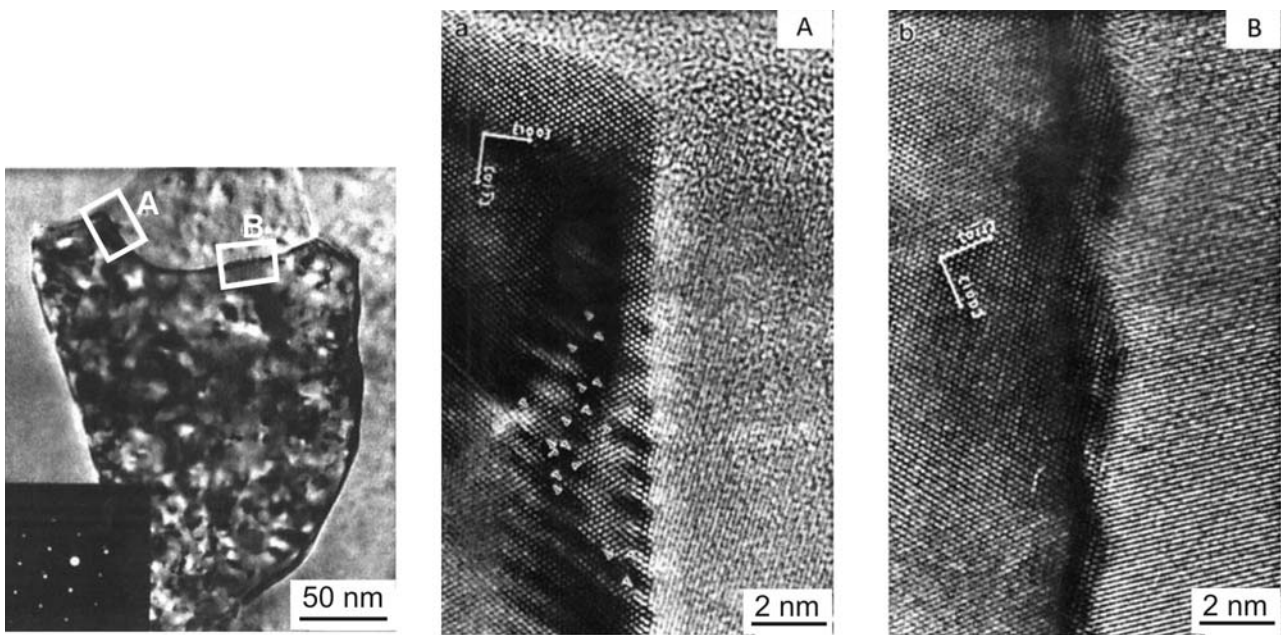

Fig. 1. TEM images of non-equilibrium grain boundaries in the UFG Al-3%Mg alloy with a grain size of ∼ 100 nm [20] illustrating high resolution photographs of regions A and B.

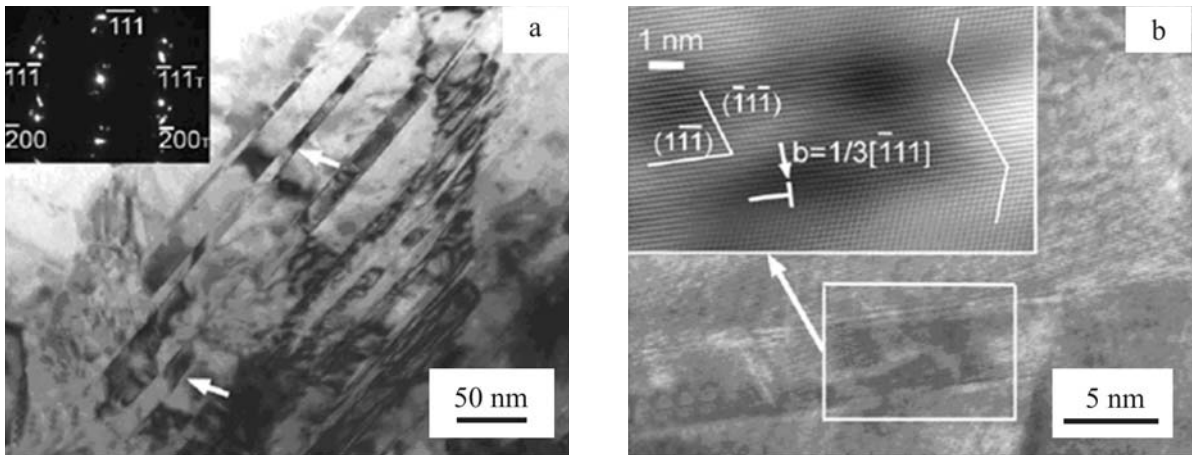

Fig. 2a,b. TEM images of a typical grain with a high density of deformation twins in UFG Cu processed by ECAP with subsequent cold rolling [23].

ever, in the process of SPD the formation of other nanostructural elements takes place as well so that dislocation substructures, twins, grain boundary segregations and precipitations also can introduce a considerable influence on the properties of these materials after processing. Moreover, representative semi-products, in the form of rods, wires and sheets, are produced by SPD processing with consequent deformation and thermal treatments may additionally refine the microstructure and influence the properties [11].

In general, in our studies four types of nanostructural elements have been identified in metals and alloys subjected to SPD that can be observed through the application of modern techniques of structural analysis such as high-resolution transmission electron microscopy (HRTEM), 3D-atom probe, etc. [4, 11, 17–20]. These elements are as follows:

3.1.1. Non-equilibrium grain boundaries

For example, as illustrated in Fig. 1 [20], an excessively high density of dislocations, facets and steps is observed at grain boundaries of the UFG alloy Al-3%Mg after HPT that leads to a non-equilibrium state of boundaries with a crystal lattice distortion zone of ∼ 5–7 nm in width [17, 21] and which considerably influences the properties of the alloy. Non-equilibrium grain boundaries are typical for different materials after SPD processing and their role in the mechanical behaviour of UFG materials has been studied in a number of reports [17, 21, 22].

3.1.2. Nanotwins, stacking faults and intragranular cells

Such nanostructural elements are typical of the materials after ECAP at lower temperatures and/or those subjected to additional cold rolling, extrusion or drawing. Figure 2 shows a TEM image of atom resolution of UFG Cu after ECAP and cold rolling at liquid nitrogen temperature with clearly observed twins of 10–20 nm in size [23]. Such nanostructured defects also have a considerable effect on material strength by, for example, increasing the yield stress in UFG Cu from ∼ 380 to ∼ 510 MPa.

3.1.3. Segregation clusters or "clouds"

Recent investigations with the application of ion microscopy and 3D-atom probe directly testify to the formation of impurity segregations and alloying elements at grain boundaries in UFG alloys processed by SPD [18, 19, 24] as shown, for example, in Fig. 3 [24]. These segregations form "clouds" or clusters ∼ 3–5 nm in size and influence the formation and motion of dislocations which accordingly leads to additional strengthening of the alloys [9, 10, 18, 24].

3.1.4. Nano-sized particles and second-phase precipitations

The formation of particles has been observed in many alloys subjected to SPD after solution quenching [11, 17]. Figure 4 illustrates an example of such nanoparticles ∼ 10–20 nm in size precipitated in the UFG alloy Al-6061 after ECAP [25]. The presence of nanoparticles is related to dynamic ageing and provides additional precipitation hardening of the alloys [11, 25].

Thus, the UFG metals and alloys processed by SPD techniques are characterized by a number of nanostructural elements that can considerably influence their properties. This is the reason that these materials are referred to as a class of "bulk nanostructured materials" and this definition has been accepted by the international community (www.nanospd.org).

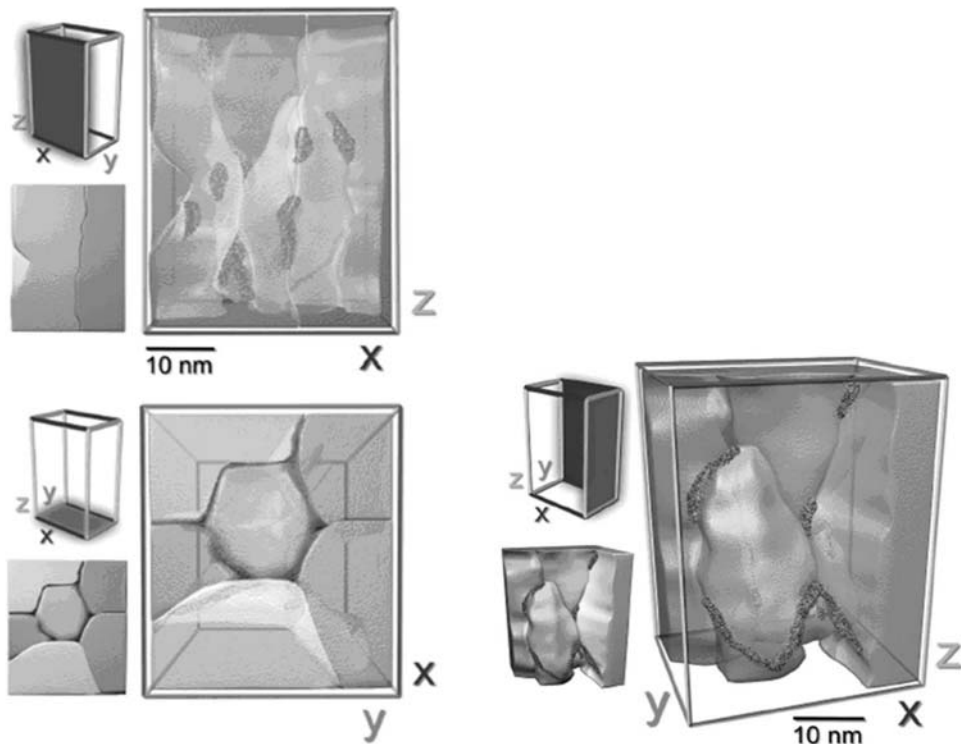

Fig. 3. Tomographic view of the nanostructure of UFG alloy Al-7075. The segregations of alloying elements are observed at grain boundaries and junctions [24].

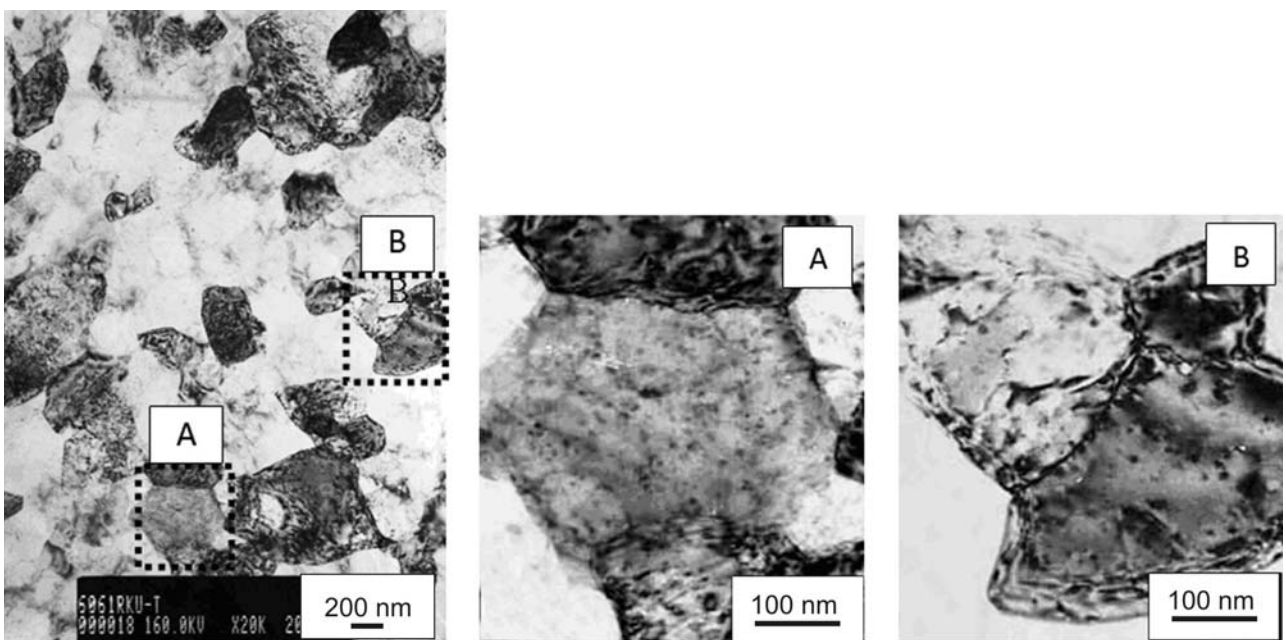

Fig. 4. UFG structure of an Al-6061 alloy after ECAP with parallel channels (4 passes): the formation of nano-sized precipitations is clearly visible inside the grain after processing [25].

It is important to note also that the strength of these materials, as shown in the following section, may be considerably higher than expected from the Hall--Petch relationship.

3.2. Observation of superstrength in UFG metals

As it was noticed above, the high strength of SPD--processed materials is usually related to the forma-

Table 1. The contribution to flow stress for SPD Ni

Processing of Ni	YS_{exp} (MPa)	YS_{calc} (MPa)	σ_{LAB} (MPa)	σ_{HAB} (MPa)	σ_{GBDs} (MPa)
ECAP + rolling	990	980	510	280	170
HPT	1200	1190	–	460	710

YS_{exp} – experimental data, YS_{calc} – calculated by means of Eq. (3)

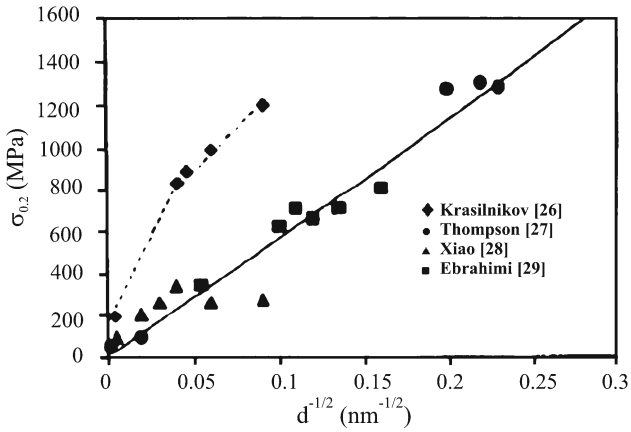

Fig. 5. Yield stress as a function of $d^{-1/2}$ for Ni: the continuous line is for material states with grains without substructure and the dashed line is for UFG Ni containing a dislocation substructure.

tion of the UFG structure via the classic Hall-Petch relationship according to which the yield stress, σ_y, is calculated as:

$$\sigma_y = \sigma_o + k_y d^{-1/2}, \tag{1}$$

where d is a grain size and σ_o and k_y are constants for the material. However, the σ_y value in UFG materials processed by SPD may be considerably higher than calculated according to the Hall-Petch relation [11].

For example, this was shown in studies of the mechanical behaviour of Ni subjected to ECAP and subsequent rolling [26]. Figure 5 shows the difference in strength between the states of Ni where the grains contain dislocation substructures within the grains and where the grains contain no substructure [27–29]. An attempt was made to describe quantitatively the deviation from the Hall-Petch rule by taking into account the influence of two types of boundaries, high-angle boundaries (HAB) between grains and low-angle cell boundaries (LAB), on the yield stress of the material. Following an earlier analysis [30], it was assumed that each of these types of boundaries, and also the nonequilibrium state of grain boundaries, contribute in an independent way to the yield stress:

$$\sigma_y = \sigma_o + \sigma_{LAB} + \sigma_{HAB} + \sigma_{NGBs} \tag{2}$$

and

$$\sigma_y = \sigma_o + M\alpha Gb((1.5S_v\theta/b)_{LAB})^{1/2} + \\ + k_y d^{-1/2} + M\alpha Gb(\rho_{GBDs})^{1/2}, \tag{3}$$

where σ_o is the threshold stress, M is the Taylor factor ($M = 3$), α is a constant ($\alpha = 0.24$), G is the shear modulus (79 GPa), b is the Burgers vector (0.249 nm), the term S_v is associated with the cell size, θ is the misorientation angle of the LAB, d is the average grain size, ρ_{GBDs} is the density of extrinsic grain boundary dislocations and k_y is the Hall-Petch constant. The numerical values for the constants were taken from the earlier report [30].

The contributions of these different components for SPD Ni correspond well to the experimentally obtained data as shown in Table 1. After HPT a homogeneous UFG structure was formed with mainly high-angle misorientations. Therefore, for the HPT sample it is reasonable to neglect the contribution of low-angle boundaries. Thus, the analysis of mechanical test data shows that the presence of substructure and the nonequilibrium state of GB contributes more strongly to the yield stress of SPD Ni than the strength calculated according to the Hall-Petch rule for a material with the given grain size.

In addition to the dislocation substructure and non-equilibrium grain boundaries, other nanostructured elements formed in the UFG materials processed

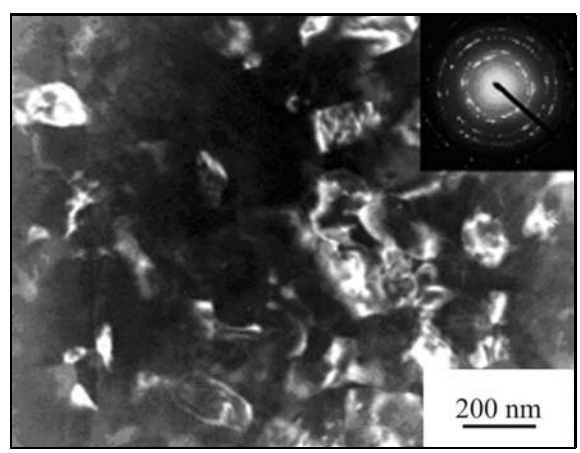

Fig. 6. Typical UFG structure formed in the alloy 1570 after HPT-processing at room temperature (dark field).

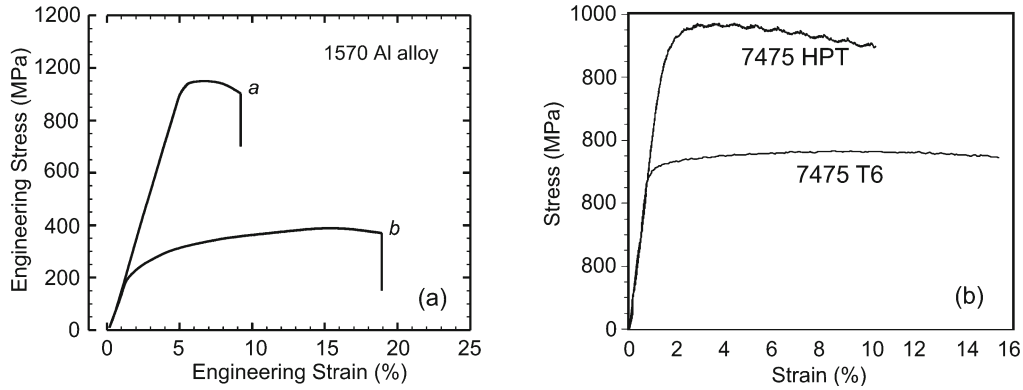

Fig. 7. Engineering stress-strain curves of the UFG alloys 1570 (a) and 7475 (b).

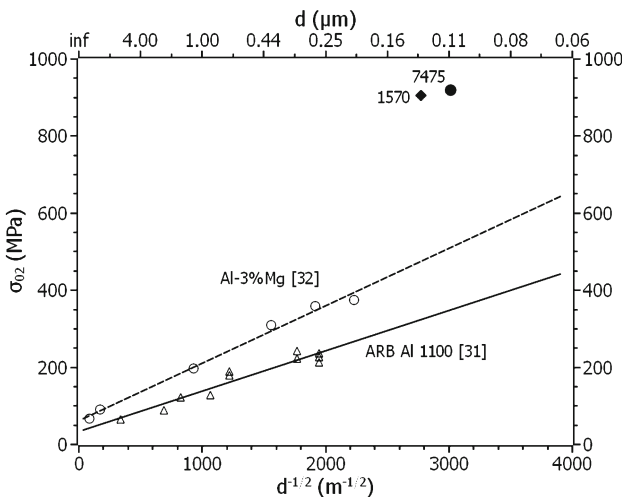

Fig. 8. The Hall-Petch relation for the alloys 1100 [31], Al-3%Mg [32] and data on the yield stresses of the UFG alloys 1570 and 7475.

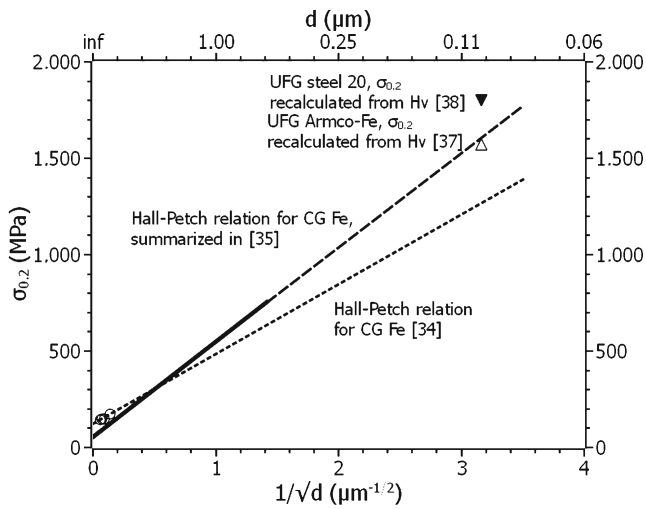

Fig. 9. The Hall-Petch relation for Armco-Fe [34] and iron [35] and data on the yield stresses of UFG Fe [14, 37] and steel 20 [38].

by SPD may contribute to the change of yield stress and flow stress. This issue was recently studied in detail for the case of super-strong UFG Al alloys, namely, Al 1570 and 7475 alloys [9, 10].

Analysis by TEM demonstrates that HPT leads to a complete transformation of the initial coarse-grained structure of the alloys into the UFG structure. In the alloys 1570 and 7475, homogeneous UFG structures with a grain size of about 100 nm are formed after HPT as shown in Fig. 6. It was also determined that HPT processing has a visible effect on the value of the crystal lattice parameter a of Al alloys. For example, in the 1570 alloy its value after straining was reduced considerably by comparison with the initial state, from 4.0765 ± 0.0001 Å to 4.0692 ± 0.0003 Å which results from the formation of Mg segregations at the grain boundaries [9, 10].

Figure 7 shows the results of mechanical testing of the 1570 and 7475 alloys. It can be seen that the UFG alloys processed by HPT at room temperature demonstrate record strength that more than twice exceeds the level of strength of the material subjected to standard hardening.

Figure 8 shows the data for a number of Al alloys presented in the form of the Hall-Petch relation in which the yield stress ($\sigma_{0.2}$) is plotted against the inverse square root of the grain size ($d^{-1/2}$) for a UFG Al alloy 1100 produced by ARB-rolling and subsequent heat treatment [31] as well as for an ECAP-processed alloy Al-3%Mg alloy [32]. For the Hall-Petch relation in the 1100 alloy [31], the following parameters were set: $\sigma_o = 6.0$ MPa and $k_y = 105$ (for the grain sizes in μm); for the ECAP-processed alloy Al-3%Mg [32], $\sigma_o = 62$ MPa and $k_y = 149$. Figure 8 also shows the data obtained for the coarse-grained (CG) and UFG 1570 and 7475 alloys.

From the available data it is seen that the σ_y values for the CG quenched alloys are close to the results for the Al-3%Mg alloy. However, for the UFG states in the 1570 and 7475 alloys with a grain size of 100–130 nm

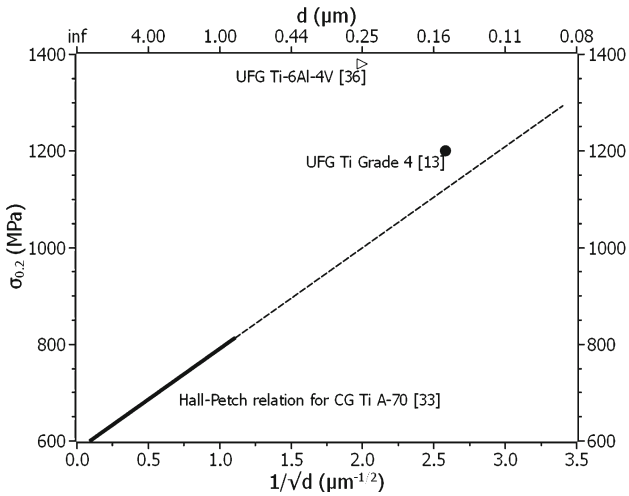

Fig. 10. The Hall-Petch relation for Ti, A-70 [33] and data on the yield stresses of UFG Ti [13] and Ti-6%Al-4%V alloy [36].

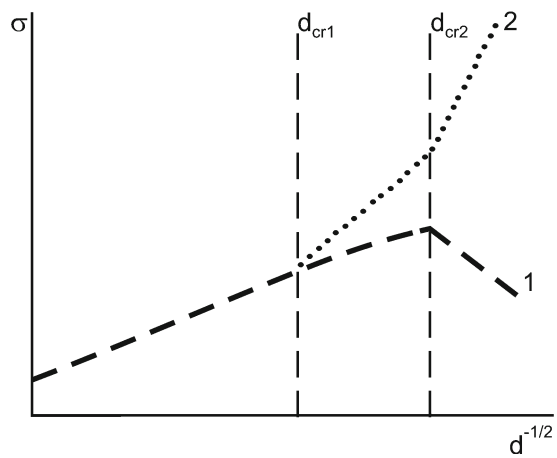

Fig. 11. Two types of the Hall-Petch slopes within different characteristic length scales [40].

the value σ_y is considerably higher than calculated from the Hall-Petch relation for these grain sizes.

The Hall-Petch plots for commercially pure (CP) Ti (A-70, similar to Grade 4) and Armco-Fe are given in Figs. 9 and 10, respectively [33–35]. Here one can also see experimental data for several UFG materials produced by SPD. In the case of CP Ti, the data are presented for HPT-processed UFG Ti-6%Al-4%V [36], and also for UFG Ti, Grade 4 processed by ECAP and further thermomechanical treatment [13]. For CP Ti it is seen that in UFG state the σ_y values are higher than could be predicted by the Hall-Petch relation for the given grain sizes. Especially a considerable excess of σ_y value is observed for the UFG alloy. For UFG Fe, the data on tensile mechanical tests are presented only in [37], but there is evidence on microhardness H_v that are demonstrated on Fig. 10 using the ratio $\sigma_y = H_v/3$. The data for HPT-processed UFG steel 20 with 0.2 % C content are also presented here [38]. As in the case with Ti, it can be observed considerable excess of experimental σ_y values (especially, for steel 20) over the values predicted from the Hall-Petch relation.

Thus, the new phenomena of super-strength of nanostructured metals and alloys, produced by SPD, can be observed for various materials. Let us discuss the nature of the phenomena in detail.

3.3. The origin of super-strength phenomena

As it was pointed out above, in recent years the Hall-Petch behaviour in the range of ultrafine grain sizes became an object for numerous experimental and theoretical studies. However, for nano-sized grains (20–50 nm) this relation is typically reported to be violated so that the Hall-Petch plot deviates from linear dependence to lower stress values and its slope k_y often becomes negative (Fig. 11, curve 1). In the present work, the examples, reflecting the "positive" slope of the Hall-Petch relation, are demonstrated (Fig. 11, curve 2).

Recently, based on experimental studies of materials obtained by vacuum depositions [39], Firstov et al. [40] reported such "positive" slope of the Hall-Petch relation, where for the grain size range $d_{cr2} < d < d_{cr1}$ the exponent of d in Eq. (1) was reported to vary from –1/2 to –1, and for $d < d_{cr1}$ the exponent of d is equal to –3 [40].

As it was shown above in this work, positive slope of Hall-Petch relation may be observed for SPD-processed metals as well. Though it is difficult to speak in terms of definite values for the exponent of d in Eq. (1) due to low statistics of experimental data, presently, however, it is possible that the presence of two characteristic grain size values is also valid for nanostructured SPD materials. Indeed, as it has been already pointed out, the presence of non-equilibrium grain boundaries is typical for the majority of SPD materials, but their influence on mechanical properties becomes considerable when the grain size is below 1000 nm. When the grain size decreases down to 100 nm and less a significant contribution of grain boundary segregations can be produced to the overall strength. Recently this question was especially addressed in [9] where it was shown that the high strength of UFG Al alloys is directly related to the formation of Mg segregations at grain boundaries revealed in the alloys by 3D APT technique [9, 24, 25]. In UFG materials deformation takes place by dislocations generated at grain boundaries and moving through a grain to be captured by an opposite grain boundary. In this case the rate-controlling mechanism is "dislocation-grain boundary" interaction. Elevated

concentration of solutes in grain boundaries can suppress emission of dislocations from such boundaries due to solute drag. Because nonuniform distribution of solutes along a grain boundary would pin a dislocation discontinuously, different regions of segregations with various Mg content will drag corresponding regions of a dislocation differently, breaking it into segments at the given stress. As a result, the characteristic length, and, correspondingly, activation volume of the deformation process will be reduced and a stress needed to emit a dislocation increases. This point is in good agreement with the experimental data and also makes it possible to explain considerably higher strength values observed in the UFG alloys in comparison with pure metals.

4. Conclusion

The conducted investigations testify to the fact that yield stress of UFG metals and alloys produced by SPD may be considerably higher than it is predicted by Hall-Petch relation for their grain size range. The observed positive slope in Hall-Petch relation provides appearance of superstrength of these materials and this is caused by nanostructural features of their grain boundaries – their non-equilibrium state and grain boundary segregations. Therefore, the problem of more detailed investigations of grain boundaries in UFG materials produced by SPD techniques is quite topical for the achievement of high strength in nanomaterials. Besides, it is important for the ongoing research to study the role of intragranular nanostructural elements – nanotwins, nanoparticles, which can lead to additional strengthening of the materials.

Acknowledgements

The Authors would like to thank the National Science Foundation of the United States (TGL) as well as the Russian Foundation for Basic Research and RF Ministry of Education and Science (RZV, NAE) for partial support of the present work.

References

[1] GLEITER, H.: Acta Mater., *48*, 2000, p. 1. doi:10.1016/S1359-6454(99)00285-2
[2] VALIEV, R. Z.—ESTRIN, Y.—HORITA, Z.—LANGDON, T. G.—ZEHETBAUER, M. J.—ZHU, Y. T.: JOM, *58*, 2006, p. 33.
[3] VALIEV, R. Z.—KRASILNIKOV, N. A.—TSENEV, N. K.: Mater. Sci. Eng., *A137*, 1991, p. 35. doi:10.1016/0921-5093(91)90316-F
[4] VALIEV, R. Z.—LANGDON, T. G.: Prog. Mater. Sci., *51*, 2006, p. 881. doi:10.1016/j.pmatsci.2006.02.003
[5] HALL, E. O.: Proc. Phys. Soc. Lond., *64B*, 1951, p. 747.
[6] PETCH, N. J.: J. Iron Steel Inst., *174*, 1953, p. 25.
[7] PANDE, C.—COOPER, K.: Prog. Mater. Sci., *54*, 2009, p. 689. doi:10.1016/j.pmatsci.2009.03.008
[8] LOUCHET, F.—WEISS, J.—RICHETON, T.: Phys. Rev. Lett., *97*, 2006, p. 75504.
[9] VALIEV, R. Z.—ENIKEEV, N. A.—MURASHKIN, M. YU.—KAZYKHANOV, V. U.—SAUVAGE, X.: Scripta Mater., *63*, 2010, p. 949. doi:10.1016/j.scriptamat.2010.07.014
[10] VALIEV, R. Z.—ENIKEEV, N. A.—MURASHKIN, M. YU.—ALEKSANDROV, S. E.—GOLDSHTEIN, R. V. : Doklady Phys., *55*, 2010, p. 267. doi:10.1134/S1028335810060054
[11] VALIEV, R. Z.—LANGDON, T. G.: Adv. Eng. Mater., *12*, 2010, p. 677. doi:10.1002/adem.201000019
[12] MURASHKIN, M. YU.—KILMAMETOV, A. R.—VALIEV, R. Z.: Phys. Met. Metallgr., *106*, 2008, p. 93.
[13] SEMENOVA, I.—SALIMGAREEVA, G.—DA COSTA, G.—LEFEBVRE, W.—VALIEV, R. Z.: Adv. Eng. Mater., *12*, 2010, p. 803. doi:10.1002/adem.201000059
[14] VALIEV, R. Z.—IVANISENKO, Y. V.—RAUCH, E. F.—BAUDELET, B.: Acta Mater., *44*, 1996, p. 4705. doi:10.1016/S1359-6454(96)00156-5
[15] KLUG, H. P.—ALEXANDER, L. E.: X-ray Diffraction Procedures for Polycrystalline and Amorphous Materials. New York, John Wiley & Sons 1974.
[16] ZHILYAEV, A. P.—LANGDON, T. G.: Prog. Mater. Sci., *53*, 2008, p. 893. doi:10.1016/j.pmatsci.2008.03.002
[17] VALIEV, R. Z.—ISLAMGALIEV, R. K.—ALEXANDROV, I. V.: Prog. Mater. Sci., *45*, 2000, p. 103. doi:10.1016/S0079-6425(99)00007-9
[18] NURISLAMOVA, G.—SAUVAGE, X.—MURASHKIN, M.—ISLAMGALIEV, R.—VALIEV, R.: Phil. Mag. Lett., *88*, 2008, p. 459. doi:10.1080/09500830802186938
[19] SHA, G.—WANG, Y. B.—LIAO, X. Z.—DUAN, Z. C.—RINGER, S. P.—LANGDON, T. G.: Acta Mater., *57*, 2009, p. 3123. doi:10.1016/j.actamat.2009.03.017
[20] HORITA, Z.—SMITH, D. J.—FURUKAWA, M.—NEMOTO, M.—VALIEV, R. Z.—LANGDON, T. G.: J. Mater. Res., *11*, 1996, p. 1880. doi:10.1557/JMR.1996.0239
[21] VALIEV, R. Z.—NAZAROV, A. A.: In: Bulk Nanostructured Materials. Eds.: Zehetbauer, M. J., Zhu, Y. T. Weinheim, Germany, WILEY-VCH Verlag GmbH & Co. KGaA 2009, p. 21.
[22] VALIEV, R. Z.—KOZLOV, E. V.—IVANOV, YU. F.—LIAN, J.—NAZAROV, A. A.—BAUDELET, B.: Acta Metall. Mater., *42*, 1994, p. 2467. doi:10.1016/0956-7151(94)90326-3
[23] ZHAO, Y.—BINGERT, J. F.— LIAO, X.—CUI, B.—HAN, K.—SERGUEEVA, A. V.—MUKHERJEE, A. K.—VALIEV, R. Z.—LANGDON, T. G.—ZHU, Y. T.: Adv. Mater., *18*, 2006, p. 2949. doi:10.1002/adma.200601472
[24] LIDDICOAT, P. V.—LIAO, X. Z.—ZHAO, Y.—ZHU, Y.—MURASHKIN, M. Y.—LAVERNIA, E.

J.—VALIEV, R. Z.—RINGER, S. P.: Nat. Commun. 1:63. doi: 10.1038/ncomms1062 (2010)
[25] VALIEV, R. Z.—MURASHKIN, M. YU.—BOBRUK, E. V.—RAAB, G. I.: Mater. Trans., *50*, 2009, p. 87.
[26] KRASILNIKOV, N.—LOJKOWSKI, W.—PAKIELA, Z.—VALIEV, R. Z.: Mater. Sci. Eng., *A37*, 2005, p. 330. doi:10.1016/j.msea.2005.03.001
[27] THOMPSON, A. W.: Acta Metall., *23*, 1975, p. 1337. doi:10.1016/0001-6160(75)90142-X
[28] XIAO, C.—MIRSHAMS, R. A.—WHANG, S. H.—YIN, W. M : Mater. Sci. Eng., *A301*, 2001, p. 35. doi:10.1016/S0921-5093(00)01392-7
[29] EBRAHIMI, F.—BOURNE, G. R.—KELLY, M. S.—MATTHEWS, T. E.: Nanostr. Mater., *11*, 1999, p. 343. doi:10.1016/S0965-9773(99)00050-1
[30] HUGHES, D. A.—HANSEN, N.: Acta Metall., *48*, 2000, p. 2985.
[31] TSUJI, N.: In: Nanostructured Materials by High-Pressure Severe Plastic Deformation. Eds.: Zhu, Y. T., Varyukhin, V. Dordrecht, Springer Netherlands 2006, p. 227.
[32] FURUKAWA, M.—HORITA, Z.—NEMOTO, M.—VALIEV, R. Z.—LANGDON, T. G.: Phil. Mag. A, *78*, 1998, p. 203. doi:10.1080/01418619808244809
[33] JONES, R. L.—CONRAD, H.: Trans. Met. Soc. AIME, *245*, 1969, p. 779.
[34] CHARIT, I.—MURTY, K. L.: Transactions, SMiRT 19, Toronto 2007, Paper # D03/3 p. 1.
[35] MALOW, T. R.—KOCH, C. C.: Met. Mater. Trans. A, *29*, 1998, p. 2285. doi:10.1007/s11661-998-0106-1
[36] SERGUEEVA, A. V.—STOLYAROV, V. V.—VALIEV, R. Z.—MUKHERJEE, A. K.: Mater. Sci. Eng., *A323*, 2002, p. 318. doi:10.1016/S0921-5093(01)01384-3
[37] IVANISENKO, YU.—SERGUEEVA, A. V.—MINKOW, A.—VALIEV, R. Z.—FECHT, H.-J.: In: Nanomaterials by Severe Plastic Deformation. Eds.: Zehetbauer, M. J., Valiev, R. Z. Weinheim, Germany, Wiley-VCH 2004, p. 453.
[38] CHUKIN, M. V.—KOPTSEVA, N. V.—VALIEV, R. Z.—YAKOVLEVA, I. L.—ZRNIK, J.—COVARIK, T.: Vestnik MGTU (Herald of MGTU), *1*, 2008, p. 31.
[39] FIRSTOV, S. A.—ROGUL, T. G.—MARUSHKO, V. T.—SAGAYDAK, V. A.: Vopr. Materialoved. (The Issues of Materials Science), *33*, 2003, p. 201.
[40] FIRSTOV, S. A.—ROGUL, T. G.—SHUT, O. A.: Functional Materials, *16*, 2009, p. 4.